Effect of Y and Ni addition on liquid immiscibility in Cu–Zr–Ag ternary alloys

Dora Janovszky[a], Kinga Tomolya[a], Maria Sveda[a], Anna Sycheva[a], George Kaptay[b]

[a] MTA-ME Material Science Research Group, Miskolc, Hungary
[b]Department of Nano-materials, Bay Zoltan Applied Research Non-Profit Ltd.
H-3519 Miskolc, Igloi 2, Hungary

[a]Corresponding author: fekjd@uni-miskolc.hu

Abstract

Liquid immiscibility was studied in Cu-Zr-Ag-Y and Cu-Zr-Ag-Ni liquid alloy systems. In case of Y addition the liquid decomposes into an Ag-Y rich liquid (L_1) and into a Cu-Zr rich liquid (L_2). In case of Ni addition the separated liquid phases are Ag-rich and Cu-Zr-Ni rich liquids. Different microstructures were found as function of the volume fraction of the L_1 liquid phase. The Y addition increased the field of miscibility gap of the ternary Cu-Zr-Ag system to a greater extent compared to Ni addition. Also, the rate of coalescence of droplets in the Cu-Zr-Ag-Y system was considerably larger compared to the Cu-Zr-Ag-Ni system. These two observations are interconnected: increased miscibility means more positive excess Gibbs energy, which leads to higher liquid/liquid interfacial energy, being the driving force of coalescence. Alloys with different compositions taken from the tip of the wedge have been studied by DSC. The amorphous fraction progressively reduces when increasing the Ag-content. A small amount of amorphous phase was detected by DSC in the alloy with Ag contents of not greater than 50 at%.

Keywords: Ag-Cu-Zr alloy, Liquid-liquid separation, Miscibility gap, Monotectic, Rapid solidification

1. Introduction

Copper-zirconium (Cu-Zr) bulk metallic glasses (BMGs) have been developed due to their lower cost compared to Zr-based BMGs [1-6]. As the BMGs are quite brittle, their further development was necessary to improve their ductility, which can be achieved in three ways: either by extrinsically adding a second crystalline phase to the amorphous matrix [7] or by intrinsic phase separation [8] or by partial nanocrystallization of the amorphous matrix [9]. It is worth noting that the second phase`s shape and morphology are also very important parameters affecting mechanical properties. The second phase with sharp edges is a stress concentration site, so it reduces toughness. In contrast a spherical second phase improves the mechanical properties. The liquid phase separation meets these requirements: i. the separated phase forms spherical, generally liquid drops; ii. the liquid drops become amorphous or crystalline. In recent years such novel amorphous/amorphous [10-13] or amorphous / crystalline [14-16] composites have been synthesized.

Our subject is the study of the liquid immiscibility in the Ag-Cu-Zr system, in which the homogenous liquid separates into an Ag-rich liquid (L_1) and into a Cu–Zr-rich liquid (L_2) during cooling through the miscibility gap [17-18]. In the present work nickel (Ni) and yttrium (Y) are separately added to the Ag-Cu-Zr system and their influence is studied on liquid immiscibility. These two alloying elements have been chosen to check the effect of the heat of mixing between silver (Ag) and the given element: the heat of mixing in the Ag-Y system is highly negative [19]) while that in the Ag-Ni system is positive [20].

2. Experimental

The master alloy ingots were prepared by arc-melting from a mixture of pure metals under purified argon atmosphere (min. 99.99 m%) with a Ti-getter. The ingots were re-melted at least four times in order to ensure chemical homogeneity. The nominal compositions of the Cu-Zr-Ag-Y and Cu-Zr-Ag-Ni alloys studied in the present work are listed in Table 1 and Table 2. The ingots were re-melted in a glassy carbon crucible by induction melting, followed by centrifugal casting into wedge-shaped copper moulds under argon atmosphere. Wedge-shaped samples (30 mm high, 6 mm thick, 6mm wide) were selected in order to achieved high cooling rate. The samples were examined by a Zeiss EVO MA and by a Hitachi S-4800 (for higher resolution images) scanning electron microscopes (SEM) equipped with an EDX energy-dispersive X-ray spectrometer.

Backscattered electron micrographs were recorded in order to get information about the composition of the phases. The thermal analysis was performed by a Netzsch 204 differential scanning calorimeter (DSC) under Ar atmosphere with a heating rate of 0.67 K/s. For 2-phase samples the volume fraction was determined by image analysis was performed by Zeiss Axio Vision Imager equipment using Leica software, while the composition of the phase with smaller volume fraction was determined by EDS analysis. These data were used to calculate the composition of the phase with a larger volume fraction using an algorithm of [18] extended to 4-component systems with molar volumes of Ag, Cu and Ni taken from [21], while molar volumes of Zr and Y taken from [22]. The results are given in Tables 1-2.

3. Results

3.1. The Cu-Zr-Ag-Y system

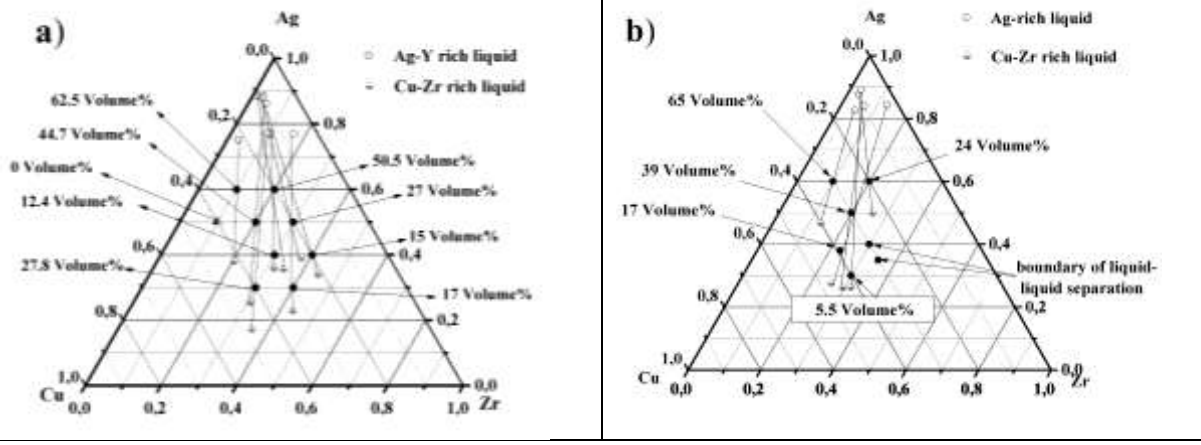

Fig.1: The pseudo-ternary Cu-Zr-Ag phase diagram in at% with 5 at% Y (a) and 5 at% Ni (b), with a miscibility gap of the liquid phase determined experimentally. Black circles show our samples with miscibility gap in master alloys, semi-filled triangles indicate our samples without miscibility gap. The red line represents the liquid miscibility gap observed in Cu-Zr-Ag system [18].

Fig.1a) shows the samples on the $(Cu–Zr–Ag)_{0.95}Y_{0.05}$ pseudo-ternary phase diagram with a constant Y content (5 at%). In samples with immiscibility the initially homogeneous liquid (L) separates into two liquids: one rich in Ag-Y (hereinafter referred to as L_1) and the other one rich in Cu-Zr (hereinafter referred to as L_2), connected with tie-lines in the pseudo ternary diagram. The addition of Y extended the boundaries of the liquid miscibility gap measured in the Cu-Zr-Ag ternary system [18].This extension is observed towards lower silver contents and higher zirconium content (Fig.1a).

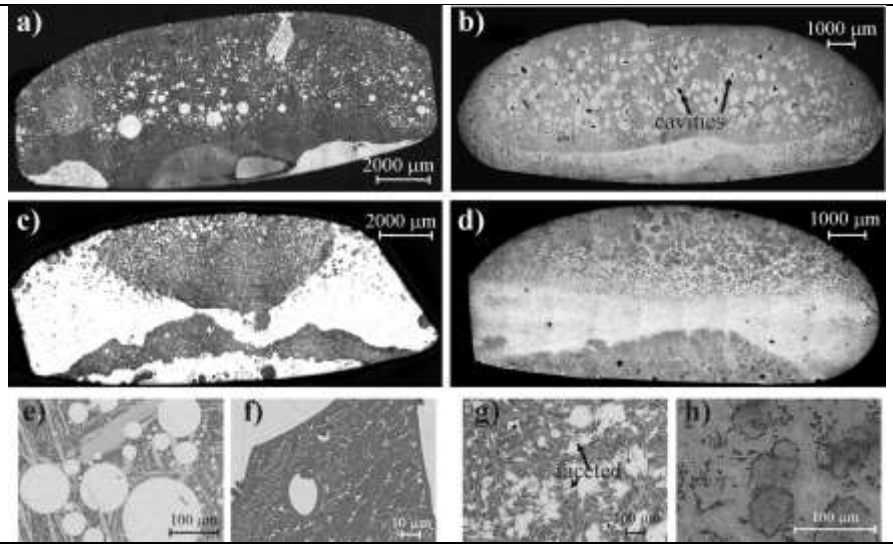

Fig.2: Optical micrographs and back scattered SEM micrographs from master alloys with different compositions in the Cu-Zr-Ag-Y system. The Ag-Y rich phase appears bright, the Cu-Zr-rich phase is dark. Samples were marked as follows: L_1 volume % / picture. $Cu_{28.5}Zr_{38}Ag_{28.5}Y_5$ (17 / a, e); $Cu_{28.5}Zr_{19}Ag_{47.5}Y_5$ (44.7 / b, f); $Cu_{19}Zr_{19}Ag_{57}Y_5$ (50.5/ c, g); $Cu_{28.5}Zr_{9.5}Ag_{57}Y_5$ (62.5 / d, h)

Two different microstructures can be distinguished during the liquid separation process as a function of volume fraction of the Ag-rich liquid (L_1):

Region 1, where L_1 has a volume fraction lower than 50%. Six samples belong to this region (see Table 1). Increasing the L_1 volume, a thicker Ag-Y-rich layer is formed at the bottom of the ingots because this phase is also heavier (Fig.2 a, b). A smaller volume of L_1 liquid migrated to the middle of the ingot (Fig.2). The rounded morphology of the Ag-Y-rich droplets in the liquid state is frozen in most cases. L_1 droplets did not solidify first in the master alloys as evidenced by the fact that some separated droplets are cut through by a phase with faceted growth morphologies (Fig.2 e) and cavities in Ag-Y rich solidified droplets. (Fig.2 b). Although the composition of L_1 droplets did not change significantly, the solidified structure changed greatly. The L_1 spheres contain 65-79 at% Ag, 7-16 at% Y and the rest Cu - Zr. Increasing the volume fraction of L_1 liquid the separated liquid lost its approximately spherical shape and became ovoid in shape (Fig.2 f). The L_2 liquid contain 31-45 at% Cu, 31-43 at% Zr and 14-34 at% Ag.

Region 2, with the L_1 phase having a fraction larger than 50 %. Only the $Cu_{28.5}Zr_{9.5}Ag_{57}Y_5$ and $Cu_{19}Zr_{19}Ag_{57}Y_5$ master alloys belong to this region. In this region, spherical droplets of the L_2 liquid are dispersed in the matrix of L_1 liquid. The cross section of master alloy demonstrates that a sandwich type structure has developed (Fig.2 c,d). Most of the Cu-Zr-rich particles are at the bottom and the top of the master alloy. In $Cu_{19}Zr_{19}Ag_{57}Y_5$ sample some L_1 droplets remained in the matrix which is cut through by a phase with faceted growth morphologies (Fig.2 g). L_2 droplets were also covered with a thin layer rich in Cu-Zr (Fig.2 h).

The Cu - Zr rich liquid can become amorphous structure during rapid cooling by copper mould casting. Fig.4a displays the DSC traces of the as-cast samples. Specimens were derived from the tip of wedge-shaped samples. Compositions exhibit wide supercooled liquid regions (ΔT_x) larger than 50 °C followed by exothermic heating process of crystallization. The amorphous phase can be formed only when the thickness of the composite sample is lower than 1.8 mm. Its fraction in the sample progressively reduces with increased Ag-content.

3.2 The Cu-Zr-Ag-Ni system

Fig.1b shows the samples on the ternary diagram. The system was considered as a $(Cu–Zr–Ag)_{0.95}Ni_{0.05}$ pseudo-ternary. In the samples with liquid immiscibility the melt (L) separated into two liquids: one is rich in Ag (hereinafter referred to as L_1) and the other one is rich in Cu-Zr-Ni (hereinafter referred to as L_2). The field of liquid immiscibility is similar to that in the ternary Cu-Zr-Ag alloy [18]. The average initial composition, the composition of two liquids and their volume fractions are given in Table 2. In this system also two different microstructures can be distinguished during the liquid separation process as a function of volume % of the Ag-rich liquid (L_1):

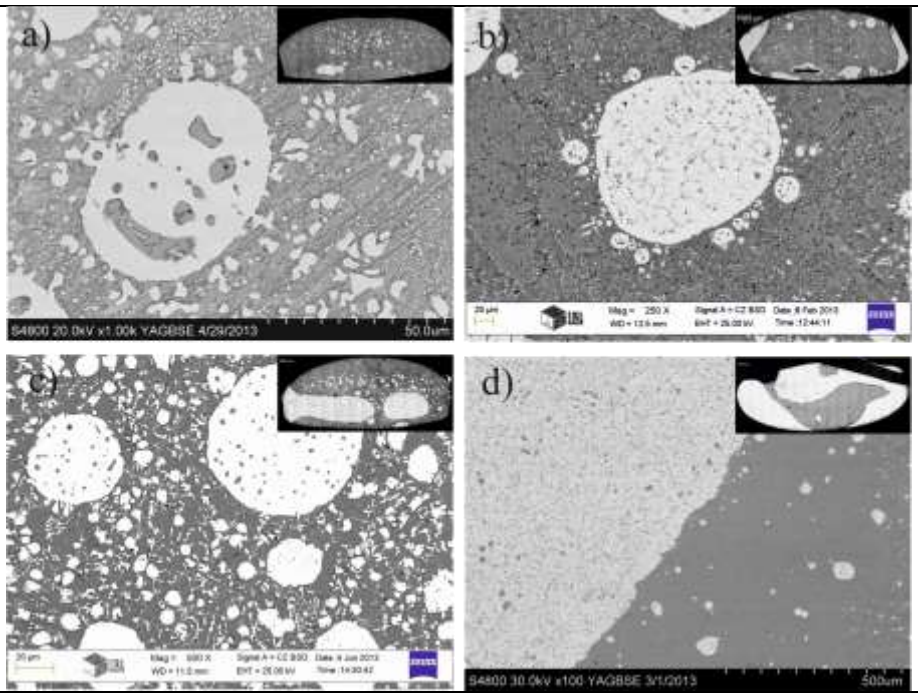

Fig.3: Optical micrographs and back scattered SEM micrographs from master alloys with different compositions in the Cu-Zr-Ag-Ni system. The Ag- rich phase appears bright, the Cu-Zr-Ni-rich one dark. Samples were marked as follows: L_1 volume % / picture. $Cu_{37}Zr_{22}Ag_{36}Ni_5$ (17.0 / a, e); $Cu_{19}Zr_{19}Ag_{57}Ni_5$ (24.0 / b, f); $Cu_{28.5}Zr_{19}Ag_{47.5}Ni_5$ (39.0 / c, g); $Cu_{28.5}Zr_{9.5}Ag_{57}Ni_5$ (65.0 / d, h)

Region 1 where L_1 has a volume fraction lower than 50%. In this region, large coagulated L_1 droplets can be observed in the middle of the samples (Fig.3a,b,c). Some L_2 droplets are frozen within the L_1 particles (Fig.3e). In the $Cu_{37}Zr_{22}Ag_{36}Ni_5$ sample the frozen collision between the moving droplets (Fig.3f,g) can be observed. The L_1 spheres contain 82-84 at% Ag, less than 1 at% Ni and 3-13 at% Cu, 4-12 at% Zr. The L_2 liquid contains 24-43 at% Cu, 23-27 at% Zr, 6-8 at% Ni and 24-26 at% Ag. These results suggest that such compositions would not have good GFA because the Zr content is too small.

Region 2 where the volume fraction of the Ag-rich liquid is larger than 50%. There is only one system like this, the $Cu_{28.5}Zr_{9.5}Ag_{57}Ni_5$ master alloy. In this system, L_2 droplets coalesced into two giant droplets (Fig.3d) Some L_1 droplets were incorporated into these huge droplets (Fig.3 h). Amorphous matrix was achieved by rapid solidification from the Cu-Zr-Ni rich liquid. The maximum thickness of amomorphous matrix was much smaller than in the samples alloyed with Y. Fig.4b displays the DSC traces of the as-cast samples.

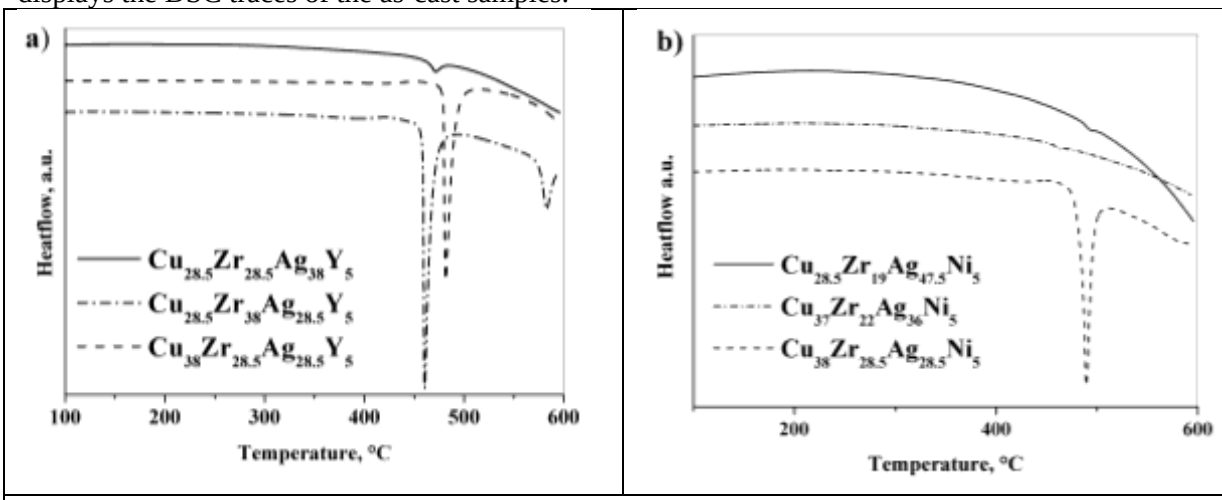

Fig.4: DSC curves of the tip of the wedge-shape samples in Cu-Zr-Ag-Y (a) and in Cu-Zr-Ag-Ni (b) systems (heating rate 0.67 °C/s)

4. Discussion

The experimental results previously reported were interpreted on the basis of the thermodynamic properties listed in Table 3. [21-23]:

1. The Ag-Cu-Zr system: the Ag-Cu sub-system is eutectic with no intermetallic compounds; the Ag-Zr sub-system has two intermetallic compounds, both relatively unstable (dissociating in peritectic reactions); the Cu-Zr has 6 intermetallic compounds, 3 of them are relatively stable (with congruent melting points). Thus, the most stable associate of the Ag-Cu-Zr system will be $CuZr_x$, which is not fully metallic, so it cannot mix perfectly with metallic liquid Ag. Therefore, the Ag-Cu-Zr liquid alloy separates into a Cu-Zr rich liquid and into an Ag-rich liquid phases.

2. The addition of Ni to the Ag-Cu-Zr system: the new Ag-Ni sub-system is monotectic, i.e. Ag and Ni atoms do not preferably mix; the new Cu-Ni sub-system shows solid solutions, i.e. Cu and Ni mix almost ideally in liquid state; the new Zr-Ni sub-system shows 7 intermetallic compounds, 3 of them are relatively stable (with congruent melting points). Thus, in the quaternary Ag-Cu-Zr-Ni system both $CuZr_x$ and $NiZr_x$ associates can form, even the formation of ternary $(Cu-Ni)Zr_x$ associates is possible (due to the almost ideal Cu-Ni sub-system). In contrary, the new component Ni does not prefer to mix with Ag. Thus, the addition of Ni to the Ag-Cu-Zr system does not change the above conclusion that two immiscible liquids form: one of them is rich in Ag, another one is not rich in Cu-Zr-Ni.

3. The addition of Y to the Ag-Cu-Zr system: the new Ag-Y sub-system shows 3 intermetallic compounds, all of them are relatively stable (with congruent melting points); the new Cu-Y sub-system shows relatively unstable intermetallic compounds (dissociating in peritectic reactions); the new Y-Zr sub-system forms an eutectic. Thus, the most stable associate brought into the system by adding Y to Ag-Cu-Zr alloy will be AgY_x. As a consequence, Y will preferably mix with Ag to form an Ag-Y rich liquid alloy. Thus, in the quaternary Ag-Cu-Zr-Y system the two separated liquids will be an Ag-Y rich liquid and a Cu-Zr rich liquid.

The coalescence of similar droplets takes place to eliminate liquid/liquid interfaces. The driving force and the rate of coalescence are proportional to the liquid/liquid interfacial energy. The liquid/liquid interfacial energy is proportional to the maximum of the excess Gibbs energy of mixing [24-27]. The latter, on the other hand, leads to more extended miscibility gap. Thus, the more extended is the miscibility gap, the higher should be the rate of coalescence. This theoretical correlation is supported by the following experimental observations made in this paper:

i. the extent of the miscibility gap is similar in the ternary Ag-Cu-Zr and in the quaternary Ag-Cu-Zr-Ni systems, while it is considerably more extended in the Ag-Cu-Zr-Y quaternary system.
ii. the rate of coalescence is similar in the ternary Ag-Cu-Zr and in the quaternary Ag-Cu-Zr-Ni systems, while it is considerably increased for the Ag-Cu-Zr-Y quaternary system. In both $Cu_{28.5}Zr_{38}Ag_{28.5}Y_5$ and $Cu_{37}Zr_{22}Ag_{36}Ni_5$ master alloys the separated L_1 volume fraction is 17 %. The percentage of area occupied by droplets larger than 0.1 mm^2 is 55.5% in Y containing sample while in Ni containing sample is 27.2%.

5. Conclusions

In this work the microstructures of Cu-Zr-Ag-Y and Cu-Zr-Ag-Ni alloys were investigated, which yielded the following results:

1. The liquid becomes immiscible within a given composition range in both Cu-Zr-Ag-Ni and in the Cu-Zr-Ag-Y systems. In case of Y addition the quaternary liquid decomposes into an Ag-Y rich liquid (L_1) and into a Cu-Zr rich liquid (L_2). In case of Ni addition the separated liquid phases are Ag-rich and Cu-Zr-Ni rich liquids.
2. The Y addition increased the field of miscibility gap to a greater extent compared to Ni addition which is in agreement with the thermodynamic analysis.
3. The rate of coalescence is higher in the quaternary Ag-Cu-Zr-Y system than in Ag-Cu-Zr-Ni systems, due to higher liquid-liquid interfacial energy (due to a more extended miscibility gap), thus due to larger driving force of droplets coalescence in the Ag-Cu-Zr-Y system, compared to the Ag-Cu-Zr-Ni system.
4. The presence of different types of structures was observed in the samples, namely typical droplet-like structures and irregular structures. The analysis of the structures as function of L_1 content yielded two clearly distinguishable structures.

5. Alloys with different compositions taken from the tip of the wedge have been studied by DSC. The amorphous fraction progressively reduces when increasing the Ag-content. A small amount of amorphous phase was detected by DSC in the alloys with Ag contents of not greater than 50 at%.

References

[1] Q. Zhang, W. Zhang, A. Inoue, Scripta Mater 55 (2006) 711–713

[2] H.M. Fu, H.F. Zhang, H.Wang, Z.Q. Hu, J. Alloys Compd. 458 (2008) 390–393

[3] T.L. Cheung, C.H. Shek, J. Alloys Compd. 434–435 (2007) 71–74

[4] W. Liao, Y. Zhao, J. He, Y. Zhang, J. Alloys Compd. 555 (2013) 357–361

[5] K.K. Song, S.Pauly, Y.Zhang, B.A.Sun, J.He, G.Z.Ma, U.Kuhn, J.Eckert, Mater. Sci. Eng. A 559(2013) 711–718

[6] W. Zhang, F. Jia, Q. Zhang, A. Inoue, Mater. Sci. Eng. A 459 (2007) 330–336

[7] S.V. Madge, T. Wada, D.V. Louzguine-Luzgin, A.L. Greer, A. Inoue, Scripta Mater 61 (5) (2009) 540–543

[8] J.C. Oh, T. Ohkubo, Y.C. Kim, E. Fleury, K. Hono, Scripta Mater, 53(2) (2005) 165-169

[9] L. Hu, F. Ye, J.Alloys Compd. 557 (2013) 160–165

[10] J. He, N. Mattern, J. Tan, J.Z. Zhao, I. Kaban, Z. Wang, L. Ratke, D.H. Kim, W.T. Kim, J. Eckert, Acta Mater 61(2013) 2102-2112

[11] J.H. Han, N. Mattern, B. Schwarz, S. Gorantla, T. Gemming, J. Eckert, Intermetallics 20 (2012) 115-122

[12] N. Mattern, T. Gemming, J. Thomas, G. Goerigk, H. Franzc, J. Eckert, J. Alloys Compd. 495 (2010) 299–304

[13] E.S. Park, J.S. Kyeong, D.H. Kim, Scripta Mater 57 (2007) 49–52

[14] C.N. Kuo, J.C. Huang, X.H. Du, X.J. Liu, T.G. Nieh, J. Alloys and Compd. xxx (2013) xxx–xxx http://dx.doi.org/10.1016/j.jallcom.2013.01.097

[15] S. González, D.V. Louzguine-Luzgin, J.H. Perepezko, A. Inoue, Mater Sci Eng A 528 (2011) 5576–5584

[16] H.Kozachkov, J.Kolodziejska, W.L.Johnson, D.C.Hofmann, Intermetallics 39 (2013) 89-93

[17] A. Castellero, D.H. Kang, I.H. Jung, G. Angella, M. Vedani, M. Baricco, J. Alloys Compd. 536 (2012) S148-S153

[18] D. Janovszky, K.Tomolya, A. Sycheva, G.Kaptay, J.Alloy Compd. 541 (2012) 353-358

[19] S.V. Ketov, L.V. Louzguina-Luzgina, A.Yu. Churyumov, A.N. Solonin, D.B. Miracle, D.V. Louzguine-Luzgin, A. Inoue, J. Non-Crystalline Solids 358 (2012) 1759–1763

[20] U.Saeed, H.Flandorfer, H.Ipser, J.Mater.Res.21 (2006) 1294-1304

[21] B.Predel: Phase Equilibria, Crystallographic and Thermodynamic Data of Binary Alloys, volume 5 of group IV of Landolt-Börnstein Handbook, Springer-Verlag, Berlin, 1991, pp.97

[22] F.R.deBoer, R.Boom, W.C.M.Mattens, A.R.Miedema: Cohesion in Metals, North-Holland, Amsterdam, 1988

[23] T.B.Massalski (ed): Binary Alloy Phase Diagrams, second ed., 3 volumes, ASM International, 1990.

[24] T.Iida, R.I.L.Guthrie: The Physical Properties of Liquid Metals, Clarendon Press, Oxford, 1993, 288 pp.

[25] G.Kaptay, Mater Sci Eng A, 495 (2008) 19-26.

[26] G.Kaptay, Calphad 32 (2008) 338-352.

[27] G.Kaptay, Acta Mater 60 (2012) 6804-6813.